

RESEARCH ARTICLE

Decoding of Brain Functional Connections Underlying Natural Grasp Task Using Time-Frequency Cross Mutual Information

HAO GU^{1,2,3}, JIAN WANG^{1,2,3}, AND YAN HAN^{1,3}¹Shanxi Key Laboratory of Signal Capturing and Processing, North University of China, Taiyuan 030051, China²State Key Laboratory for Electronic Testing Technology, North University of China, Taiyuan 030051, China³School of Information and Communication Engineering, North University of China, Taiyuan 030051, China

Corresponding authors: Jian Wang (wangjian@nuc.edu.cn) and Yan Han (9036944@qq.com)


This work was supported in part by the National Natural Science Foundation of China under Grant 62122070 and Grant 61971381, and in part by the Natural Science Foundation of Shanxi Province under Grant 20210302124190 and Grant 20210302124191.

ABSTRACT The purpose of using electroencephalogram to explore the dynamic changes of brain functional connectivity during natural grasping tasks is to uncover the underlying mechanisms of information transmission between different brain regions during cognitive processing. This exploration aims to provide new insights for the development of brain-computer interface technology and contribute to the diagnosis and treatment of brain disorders. In this study, we used time-frequency cross mutual information to evaluate the brain functional connectivity during 3-class natural grasping tasks (palmar grasp, lateral grasp and rest state). Specifically, our analysis focused on the functional brain connectivity generated by the amplitude and phase of electroencephalogram signals within the alpha (8-13 Hz) and beta (20-30 Hz) frequency bands. To assess the differences in global coupling strength, we employed two-series correlation coefficients, between different motor periods and between different brain regions for the three motor tasks. Furthermore, it was compared that the differences in the global coupling strength between different motor periods in the same motor task. Finally, the analysis of topologic characteristics in brain functional connectivity networks between the three tasks was investigated. The findings of our study indicate that functional reorganization of frontal region closely related to external visual stimuli occurs during the motor preparation period. The onset of movement leads to a lateralized reorganization of brain functional connectivity, which is associated with the right or left of the executive hand. Both the central and parietal regions contribute prominently to motor execution, and the parietal region in particular plays an important role in the execution of fine motor movements. Further analysis revealed that it is the brain's dynamic regulation of functional connectivity across frequency bands, amplitudes and phases, enabling it to perform multiple tasks with limited energy resources.

INDEX TERMS Brain functional connections, electroencephalography, time-frequency cross mutual information, natural grasping task.

I. INTRODUCTION

The brain is a highly complex system that can be divided into several brain regions with different functions. Well-established functional connectivity patterns between brain regions enable the brain to efficiently differentiate and inte-

The associate editor coordinating the review of this manuscript and approving it for publication was Md. Kafiul Islam .

grate information, leading to effective cognitive processing [1]. Consequently, investigating the functional connectivity relationships between these brain regions can offer valuable insights into how information is transmitted within the brain complex network. It also unveils the cognitive mechanisms underlying the brain, and provides new perspectives and tools for the diagnosis and treatment of neurological diseases.

Currently, there are three commonly used signals to investigate functional brain network connectivity: Magneto-Encephalo-Gram (MEG), functional Magnetic Resonance Imaging (fMRI), and Electro-Encephalo-Gram (EEG) [2], [3], [4], [5], [6]. MEG is characterized by a high temporal resolution, enabling precise tracking of brain activity. But it is more susceptible to magnetic field interference [7], [8]. With a low temporal resolution, fMRI can only reflect blood flow changes over several seconds to tens of seconds. And it cannot directly measure neuronal activity [9], [10], [11], [12]. Additionally, due to equipment limitations, MEG and fMRI need to be measured in a specific environment and are more demanding for subjects. Consequently, they may not fully reflect the functional brain connectivity during daily life. In contrast, high temporal resolution of EEG can capture changes in EEG activity at the millisecond level, which can quickly reflect the dynamic processes of the brain [13], [14], [15], [16], [17], [18]. Moreover, EEG instruments are relatively affordable and portable, facilitating measurements in laboratories, hospitals, or even at home, providing a more naturalistic assessment of dynamic brain processes.

For the same signal, there are differences in the brain functional connectivity generated by different research methods. Correlation coefficient can be used to measure the linear correlation between signals in a simple way, but it falls short in evaluating their nonlinear characteristics. Coherence reflects the linear correlation across different frequencies, except that it cannot capture the nonlinear characteristics and time-domain correlation variation between signals [19], [20], [21]. While Phase-Locked-Value (PLV) can assess the stability of phase difference between signals, it lacks sensitivity to signal amplitude, thus unable to indicate amplitude coupling between signals [22]. The Granger-Causality (GC) employs a time series model to gauge causal relationships between signals, with the assumption that the signals adhere to a Gaussian distribution. And it is sensitive to parameter selection and ignores the frequency domain characteristics [23]. Transfer-Entropy (TE) can identify non-linear causal relationships between signals, which cannot account for the time-frequency information of signals, but can be computationally complex [24], [25], [26], [27]. In contrast, the Time-Frequency-Cross-Mutual-Information (TFCMI) addresses the limitations of the aforementioned approaches. TFCMI leverages the time-frequency domain characteristics of signals and considers both signal amplitude and phase information. By evaluating both linear and nonlinear correlations between signals, TFCMI facilitates a more accurate and comprehensive construction of brain functional connectivity [28], [30].

The objective of this study was to explore the dynamic reorganization mechanism of brain functional connectivity during grasping tasks. To decode the process of dynamic change in brain functional connectivity during motor activity, we used the TFCMI to determine the coupling strength between different brain regions across various motor periods

of grasp. These coupling strengths were then compared with the default connectivity pattern observed during the rest state. To evaluate the disparity in coupling strength between brain functional connectivity during different grasp tasks and the default connectivity pattern at rest, a two-series correlation coefficient was utilized. Furthermore, the variability of coupling strength across different motor periods during the task was also assessed. Ultimately, the brain functional connectivity networks, which were generated by signal amplitude and phase information, were visualized for the different motor periods.

II. METHOD

A. PRINCIPLE OF TFCMI

TFCMI is an information-theoretic-based research method that does not rely on the assumption of a specific probability distribution for the signals [29], [30], [31], [32]. By using it to analyze the brain functional connectivity, it allows for a more precise assessment of the dynamic functional connectivity processes between different brain regions. Moreover, TFCMI has the capability to capture connectivity patterns that may be challenging to detect using traditional methods, providing a more comprehensive explanation of the reorganization process within the brain functional connectivity during motor tasks.

Morlet wavelet is a wavelet function known for its exceptional time-frequency localization properties. Using it to analyze EEG, the time-frequency band information of EEG can be well extracted, enabling a thorough understanding of the transient changes occurring in the brain during motion [33]. Furthermore, Morlet wavelet can directly extract the amplitude and phase information of EEG, thus providing a more comprehensive view of the synchronization between different brain regions during motion. Mutual information, on the other hand, is an information-theoretic metric used to quantify the extent of nonlinear dependence between signals. It does not rely on assumption about the probability distribution of signals and is particularly adept at capturing the complex dynamics features of signals. Consequently, applying it to EEG can yield a more accurate depiction of the information flow processes between different brain regions during movement. The principle underlying TFCMI involves first obtaining the amplitude and phase information of signal through wavelet transform. Subsequently, mutual information is employed to assess the potential dependencies between signals within a specific frequency band. By combining these techniques, TFCMI allows for a more precise investigation of the information flow dynamics between different brain regions during motion.

Let $x_i(t)$ denote the data from the i th channel at time instant t . The corresponding Morlet wavelet transformation is given by

$$W_{x_i}(t, f) = \int x_i(\lambda) \cdot \overline{\phi_{t,f}(t - \lambda)} d\lambda$$

where $W_{x_i}(t, f)$ represents the amplitude or phase information in frequency f of the i th channel at time instant t .

The Morlet wavelets are

$$\phi_{t,f}(\lambda) = \left(\sigma\sqrt{2}\right)^{-1/2} e^{i2\pi f(\lambda-t) - \frac{-(\lambda-t)^2}{2\sigma^2}}$$

where their time spread is defined by $\sigma = \frac{8}{2\pi f} \cdot \overline{\phi_{t,f}(\lambda)}$ are the complex conjugates of $\phi_{t,f}(\lambda)$.

Denote the averaged amplitude or phase at the i th channel by a random variable F_i , and its probability density function (pdf) by $P(F_{i,b})$. Similarly, the joint pdf between the i th and j th EEG channels were computed as $P(F_{i,b}, F_{j,b})$. The TFCMI between two random variables F_i and F_j was then calculated as follows:

$$TFCMI(F_i, F_j) = \sum_{b=1}^n P(F_{i,b}, F_{j,b}) \ln \frac{P(F_{i,b}, F_{j,b})}{P(F_{i,b})P(F_{j,b})}$$

where b represents the index of sampling bins used to construct the approximated pdf. It is crucial to estimate the pdf and joint pdf from the data histogram to calculate the mutual information [34]. When performing EEG analysis, 40 to 60 bins were used to construct the histograms.

The TFCMI matrix is reciprocal in nature with its elements indicating the strength of mutual coupling between EEG electrodes. To facilitate a clearer observation of the interdependence between channels, the matrix is normalized using the diagonal values. According to the distribution of electrodes in brain regions, the cumulative coupling strength of all electrodes in the same brain region was averaged, to gain insights into the information transfer processes between brain regions during motor tasks. The resulting averaged values represent the mutual coupling strength between these brain regions, offering a valuable insight into the information flow between them during motor tasks. Furthermore, by averaging the cumulative coupling strength of all electrodes, the global coupling strength of the brain can be obtained, which shows the dynamic reorganization process of the brain during motor activities.

B. EVALUATION INDICATORS

1) COUPLING STRENGTH DIFFERENCES

The two-series correlation coefficient is a statistical metric employed to quantify the variability between variables [35]. The larger the value, the greater the coupling difference between the variables. Applying this metric to analyze the results of TFCMI, it becomes feasible to quantify the variability of coupling strength of functional connectivity between brain regions in different motor periods. It is also advisable to assess the coupling strength variability between the motor tasks and the default connectivity patterns in the rest state. This comparative analysis provides a better understanding of the information exchange process between brain regions during motor activity. The two-series correlation coefficient

is defined as follows:

$$X_r(i, j) = \frac{\sqrt{N_{S1} \cdot N_{S2}}}{N_{S1} + N_{S2}} \cdot \frac{\text{mean}(TFCMI_{S1,m}(i, j)) - \text{mean}(TFCMI_{S2,n}(i, j))}{\text{std}(TFCMI_{S1,m}(i, j) \cup TFCMI_{S2,n}(i, j))}$$

where, $i = 1, 2, \dots, 10$ represents different brain regions, $j = 1, 2, \dots, 13$ denote different target regions. The terms $S1$ or $S2$ represent one of the palmar grasp, lateral grasp and rest state when measuring the difference between different grasp activities. While they indicate one of the movement preparation, movement onset, grasp onset, grasp holding on, and movement end, respectively, when evaluating the difference between different period of the same grasp task. $m = 1, 2, \dots, N_{S1}$ and $n = 1, 2, \dots, N_{S2}$ represent the number of trials for the two different states, $S1$ and $S2$, respectively.

2) BRAIN FUNCTIONAL CONNECTIVITY NETWORK

The brain functional connectivity network is established based on the hypothesis that brain regions with similar functions exhibit synchronized signal changes over time while performing tasks, reflecting the functional connectivity. This network provides insights into the reorganization process of the brain during higher cognitive functions. Typically, brain functional connectivity networks are usually mapped according to the degree of coupling of signals between brain regions. The elements of the TFCMI matrix represent the connection weights between brain regions, also known as the adjacency matrix. To complete the mapping of brain functional connectivity networks, either the upper triangular or lower triangular matrix is used, taking into account reciprocity. Moreover, to eliminate the occurrence of self-connections, all diagonal elements are set to zero. A specific threshold is selected, and the weights in the adjacency matrix that fall below this threshold are set to zero, yielding the weight matrix for the functional connectivity network between brain regions is obtained [36], [37]. In this study, a 60% proportion threshold was utilized to preserve network connections, allowing for the observation of distinctions among different states. Subsequently, the weight matrix is employed to visualize the functional connectivity network. During the visualization process, thicker connection lines and more pronounced colors are used to represent higher weights. In addition, Moreover, the diameter and color of a node in the network correspond to the complexity of its connection relationships with other nodes. The coupling relationships and network connections between brain regions tend to remain relatively stable state during the rest state, which is referred to as the Default-Mode-Network (DMN) [38], [39].

III. DATA AND PRE-PROCESSING

The data supporting the findings of this study was obtained from Institute of Neural Engineering, Graz University of Technology [40]. During the experiment, subjects

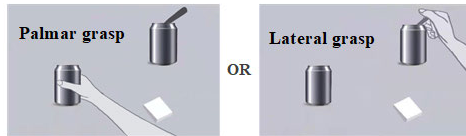


FIGURE 1. Experimental paradigm for grasp tasks.

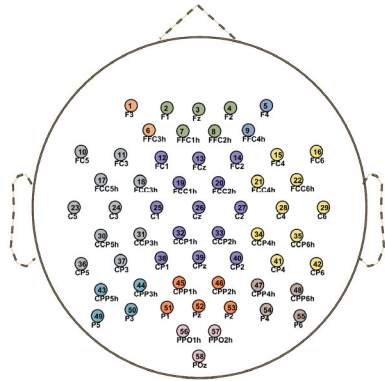


FIGURE 2. Distribution of EEG electrodes.

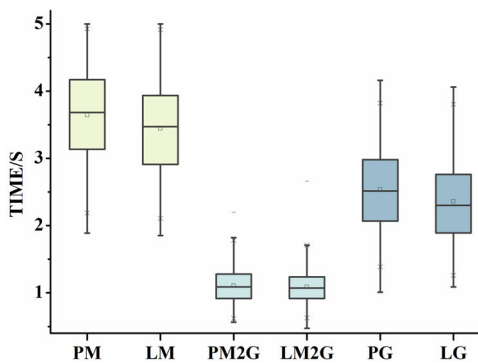


FIGURE 3. Time statistics of each period in the experimental paradigm.

autonomously grasped objects, empty cans (palmar grasp) or cans containing spoons (lateral grasp), which were equidistant from them (see Figure 1). It was required that the subjects focused their gaze on the grasped object for 1 to 2 seconds before initiating the grasping activity. They were also instructed to maintain the grasping behavior for 1 to 2 seconds after completing the grasp. Three types of EEG signals were recorded during this experiment: palmar grasp, lateral grasp and rest state. The data was collected from a group of 15 healthy subjects, all of whom were right-handed. For each subject, 58 channels of EEG signals and 6 channels of Electro-Oculo-Gram (EOG) signals (inferior and superior orbits of the left and right eyes, as well as the external eye corners) were acquired. The data were sampled at a frequency of 256 Hz with the right earlobe used as the reference electrode and the electrode AFz serving as the ground. The electrode distribution for the 58 channels is depicted in Figure 2.

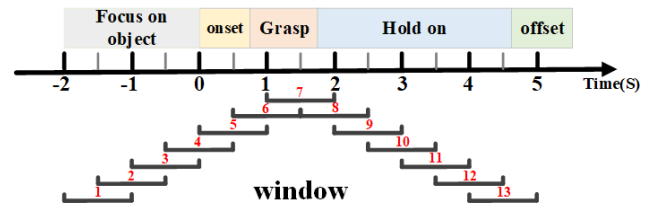


FIGURE 4. 13 segments target area in the study window.

TABLE 1. Distribution of electrodes in each brain region.

Cortical location	Channels
Left-Frontal (LF)	F3, FFC3h
Middle-Frontal (MF)	F1, FZ, F2, FFC1h, FFC2h
Right-Frontal (RF)	F4, FFC4h
Left-Central (LC)	FC5, FC3, FCC5h, FCC3h, C5, C3, CCP5h, CCP3h, CP5, CP3
Middle-Central (MC)	FC1, FCz, FC2, FCC1h, FCC2h, C1, Cz, C2, CCP1h, CCP2h, CP1, CPz, CP2
Right-Central (RC)	FC4, FC6, FCC4h, FCC6h, C4, C6, CCP4h, CCP6h, CP4, CP6
Left-Parietal (LP)	CPP5h, CPP3h, P5, P3
Middle-Parietal (MP)	CPP1h, CPP2h, Pz, P1, P2
Right-Parietal (RP)	CPP4h, CPP6h, P4, P6
Occipital (O)	PPO1h, PPO2h, POz

There was no strict time restriction on the movement duration for each period during the experiment, as the subjects were required to autonomously perform the grasp tasks, resulting in variations in execution time among individuals. In this study, statistical analysis of the movement duration was performed for each period of each trail, as illustrated in Figure 3. According to the statistical results, a study window of $[-2, 5]$ seconds relative to the movement onset was selected for further analysis. For the rest data, a window of 7 seconds with an interval of 0.5 s was used. In total, 1017 valid trials were extracted from the 15 subjects.

To observe the dynamic processes within each brain region during the grasp task, it is not ideal to have an excessive number of functional connections. Therefore, in this study, the 58-channel EEG electrodes were divided into 10 brain regions, as outlined in Table 1. Moreover, in order to gain a better understanding of the dynamic changes in brain functional connectivity throughout the entire grasp task, particularly the subtle changes during the transition between actions, the study window was further divided into 13 segments with a data overlap of 0.5 seconds, as depicted in Figure 4. As a result, the final data matrix obtained for analysis is $10 \times 13 \times 256 \times 1017 \times 3$, representing the 10 brain regions, 13 segments, 256 sampling points, 1017 trials, and 3 states of palmar grasp, lateral grasp, and rest state.

EEG are weak signals which are easily susceptible to various forms of interference, such as baseline drift, breath interference, and electrooculographic artifacts. Therefore, it is necessary to preprocess the acquired signals to obtain as clean data as possible. In this study, a 4th-order Butterworth bandpass filter with a passband range of 0.3 to 40 Hz was applied to the raw EEG. Additionally, the reference was transformed into an average reference to mitigate the lateralization bias effect. To reduce the interference of the EOG, independent components that are highly correlated with the EOG were identified and filtered out Utilizing the fast independent component analysis algorithm based on negative entropy maximization [41]. Furthermore, Laplace spatial filtering was employed to address the issue of volume conduction effects, which could potentially confound the interpretation of functional connectivity and obscure the true connectivity between brain regions [42]. This spatial filtering technique helps to restore the genuine connectivity patterns while also emphasizing local information from the channels of interest and reducing the influence of shared noise within each channel.

IV. RESULTS

This paper investigates the brain functional connectivity, generated by the amplitude and phase, between different brain regions using TFCMI analysis in two frequency bands: 8-13 Hz and 20-30 Hz. The coupling differences between palmar grasp, lateral grasp, and the rest state were assessed in various motor periods and in different brain regions using the two-series correlation coefficients. Moreover, it also compared the global coupling strength differences between different motor periods in the same motor task. Eventually the brain functional connectivity network generated by amplitude and phase was visualized, providing a graphical representation of the connections between brain regions.

A. COUPLING STRENGTH DIFFERENCE

The results depicted in Figure 5 illustrate the differences in coupling strength between three motor tasks across various periods of movement, with Figure 5a utilizing magnitude information and Figure 5b utilizing phase information. In Figure 5a, it can be observed that in the alpha band, there is a decrease in coupling strength during the preparation period (1 to 3), reaching a minimum at the onset of movement (4). However, a significant increase is observed at the initiation of the grasp (6) and during the grasp-holding period (8). On the other hand, it showed a gradual increase in the beta band. While the overall difference between the two motor tasks is small, some discrepancies can be seen in the alpha band, particularly at the onset of grasping (6) and during the grasp-holding period (8), as highlighted in Figure 5b.

For both amplitude and phase coupling strength, a significantly larger differences were observed between the rest state and the two motor tasks during various periods of movement, compared to the differences between the two motor tasks. The coupling strength differences between rest and motion states

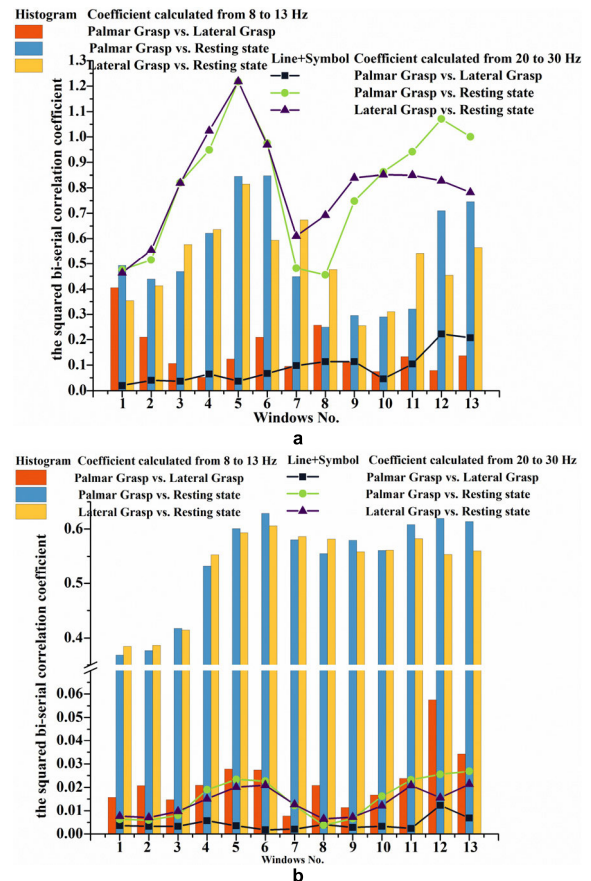


FIGURE 5. Difference in coupling strength between three motor tasks across various periods of movement.

showed an increasing trend during the preparation periods (1~3) and reached their peak at the onset of movement or grasping (4~6). During the grasping holding period (8), the differences decreased, and they increased again during the end of movement, eventually stabilizing. In addition, in terms of amplitude coupling strength, the difference between the rest state and the two motor tasks was higher in the beta band compared to the alpha band at most motor periods. Conversely, in phase coupling strength, the difference between the rest state and the two motor tasks was higher in the alpha band compared to the beta band in most motor periods.

Figure 6 illustrates the coupling strength differences between three tasks across ten brain regions, where Figure 6a utilizes amplitude information and Figure 6b utilizes phase information. It can be seen from Figure 6a that the differences between the two grasp tasks were higher in the alpha band than in the beta band in most brain regions. Within the alpha band, the differences between the grasp tasks were primarily observed in the occipital region (O), right parietal region (RP), left parietal region (LP) and left central region (LC). While within the beta band, there were more significant in the left parietal region (LP) and frontal region (F). Furthermore, as shown in Figure 6b, it can be seen that the differences between grasping tasks were mainly observed in the occipital

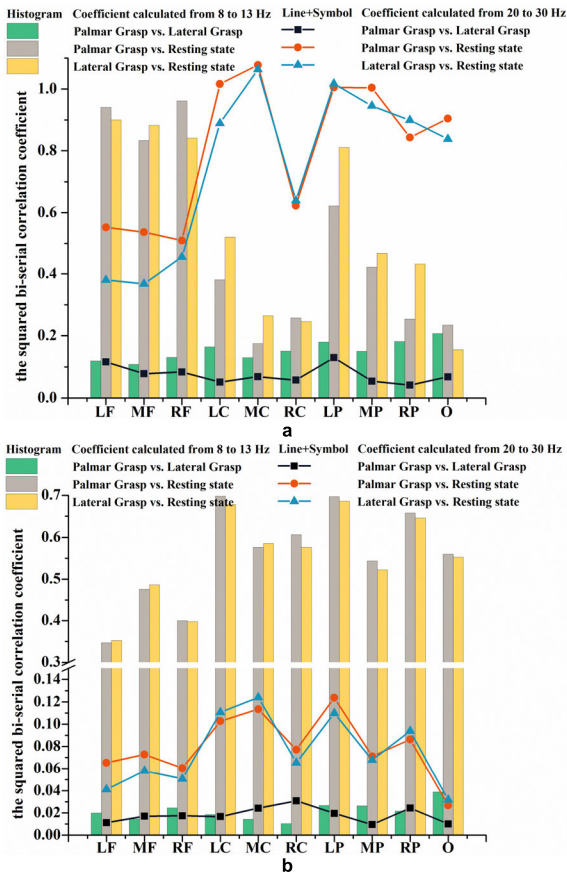
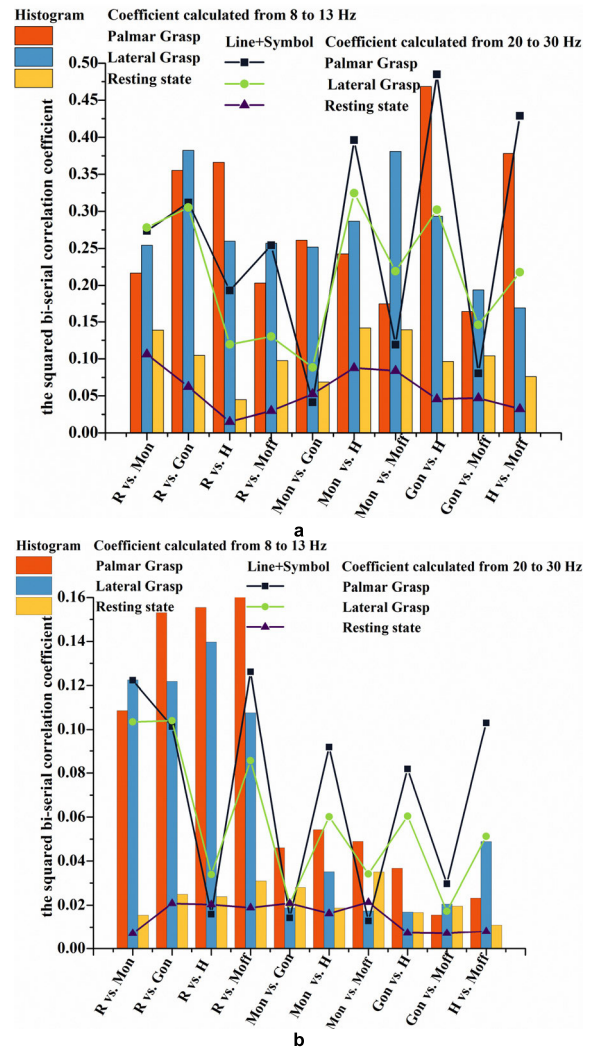


FIGURE 6. Differences in coupling strength across ten brain regions between three tasks.

region (O), parietal region (P) and right frontal region (RF) in the alpha band. In turn, more pronounced were found in the central and right side of the central region (MC, RC) and the left and right side of the parietal region (LP, RP) in the beta band.

In different brain regions, the coupling strength differences between the rest state and both motor states were significantly larger than those between the two motor states. As observed in Figure 9a, in the alpha band, the differences between the rest state and the motor state were notably pronounced in the frontal (F), left parietal (LP) and left central (LC) regions. In contrast, in the beta band, it is the left and middle central regions (LC, MC), parietal regions (P) and occipital regions (O) that show more significant variability. Whereas there were more significant differences in the beta band for the left and middle of the central region (LC, MC) and the left and right side of the parietal region (LP, RP).

Figure 7 illustrates the differences in coupling strength between five motor periods within the three tasks, where the magnitude information is used in Figure 7a and the phase information is used in Figure 7b. Both in terms of amplitude and phase, the coupling strength differences between the different movement periods of the rest state were more stable and noticeably smaller compared to the two movement states.



[Note] R, Mon, Gon, H and Moff denote the preparation state, movement onset, grasp onset, grasp hold and movement off, respectively

FIGURE 7. Difference in coupling strength between five motor periods.

As depicted in Figure 7a, the largest difference occurred between palmar grasp onset and hold, evident in both alpha and beta band. Whereas between onset of movement and grasp was the smallest, specifically in the beta band. As seen in Figure 7b, significant differences were observed between the preparation period and other moments in both movement states, surpassing the differences between movement moments within the alpha band. Meanwhile, the coupling differences between the onset of movement and the holding period, as well as between the onset of grasp and the holding period, exhibited significantly higher in the beta band compared to in the alpha band.

B. BRAIN FUNCTION CONNECTIVITY NETWORK

The functional brain connectivity networks using amplitude information, for the different movement periods of the three states are illustrated in Figure 8, with Figure 8a representing

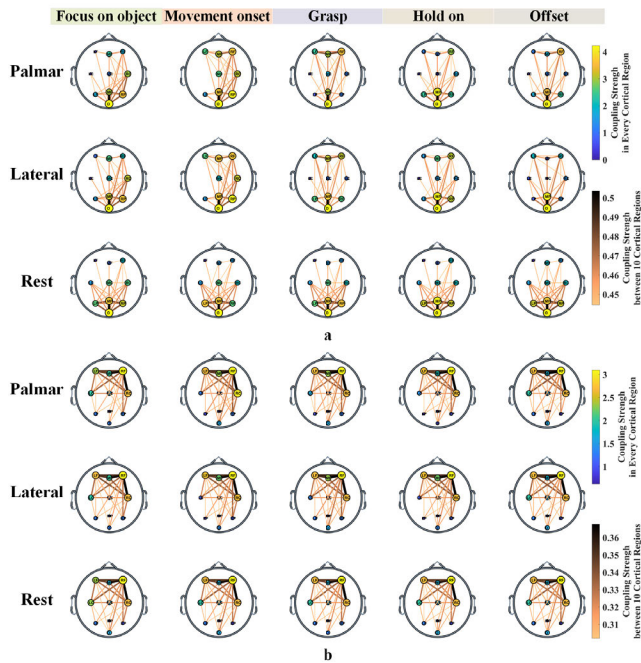


FIGURE 8. Brain functional connectivity network using amplitude information.

the alpha band and Figure 8b representing the beta band. It can be seen from Figure 8a that, in the alpha band, the connectivity networks between occipital and parietal regions, between occipital and central regions, as well as between the central and right sides of occipital and frontal regions were consistently observed. Throughout the entire movement, the connectivity strength on the left side of the central region remained at a low level. And the connectivity network, during all periods of the rest state, was primarily located in the central, parietal and occipital regions. After the onset of movement, there was a persistent network of connections between the left and right sides of the frontal regions. Compared with the rest state, the network connection between the left side of the central region and the occipital region weakened during the preparation periods of movement. At the initiation of movement, the connectivity network between the left side of the central region and the occipital region, the right side of the central region and the left side of the parietal region, further weakened, while the counterpart between the right side of the frontal region and the middle of the central region, as well as the left side of the frontal region and the left side of the parietal region, strengthened. Notably, at the onset of grasp, the connections between the left side of the central region and the occipital region, the right side of the frontal region and the left side of the parietal region, and the left side of the frontal region and the middle of the parietal region were strengthened, whereas between the right side of the central region and the middle of the parietal region weakened. At the same time, no connections were observed between the different brain regions in the central region. Remarkably, the connections between the left side of the frontal region and the left and

middle of the central region, as well as between the middle of the frontal region and the right side of the central region were specific to palmar grasp, whereas between the left side of the parietal region and the left and middle of the frontal region were specific to lateral grasp. During the hold period of grasp, the connection between the right side of the central region and the middle of the parietal region was enhanced. In addition, the strength of the connections in the frontal region decreased, while the strength of the connections in the parietal region increased. At the end of the movement, there was an enhanced connection between the left side of the central region and the left side of the parietal region.

As depicted in Figure 8b, in the beta band, the connection strength was highest in the right side of the frontal region. During the rest state (excluding the end of movement), there were ongoing connectivity networks within the central region and between the left side of the frontal region and the occipital region. In comparison to the rest state, during the preparation period of movement, the connectivity strength of the left side of the central region begins to decrease. At the onset of movement, the strength of functional connections in the left side of the central region and in the occipital region decreased. Additionally, the connectivity between the left side of the central region and the middle of the central region, as well as between the left side of the central region and the left side of the occipital region, weakened. However, the functional connections on the left side of the central region increased at the onset of grasp. Specifically, the connection between the left side of the central region and the left side of the parietal region was enhanced for palmar grasp compared with lateral grasp. There was a decrease of connectivity in the parietal region during the hold of grasp. At the end of the movement, there is a disappearance of the connectivity network between the middle part of the central region and the middle part of the parietal region.

Figure 9 illustrates the brain functional connectivity network based on the phase information for the different motor periods of the three tasks, where Figure 9a shows the alpha band and Figure 9b shows the beta band. As seen in Figure 9a, in the alpha band, it could be consistently observed that the network connections between the middle frontal region and the left side of the central region, between the middle frontal region and the left side of the parietal region, as well as between the occipital region and the left side and right side of the central region during the resting state. The connections between the left side of the frontal region and the right side of the parietal region could be observed throughout the motor status. Following the initiation of movement, the connections between the left side of the frontal region and the left side of the parietal region remained present. With respect to the rest state, the network connections between the left side of the central region and the occipital region weakened during the movement preparation period. The connection strength on the left side of the central region was enhanced at the onset of movement. Nevertheless, at the onset of grasp, there is a weakening of the connection between

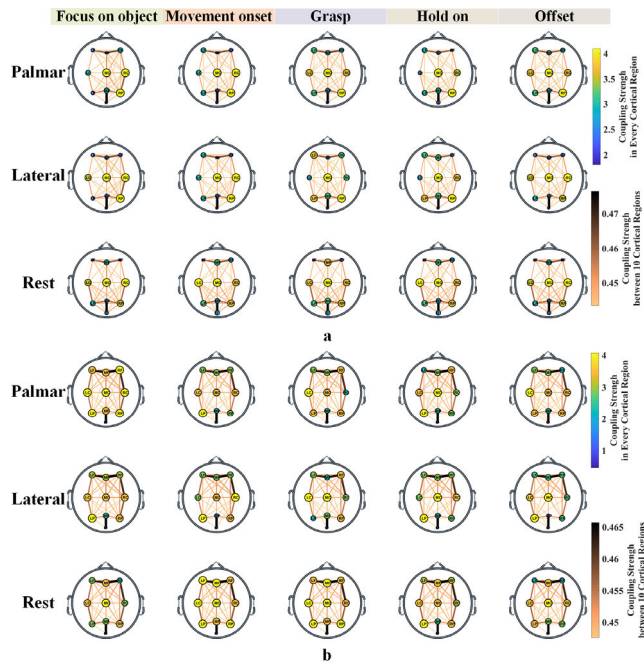


FIGURE 9. Brain functional connectivity network using phase information.

the right side of the central region and the occipital region. It is of interest that the strength of connections in the central region was significantly higher for palmer grasp compared to lateral grasp. During the grasp-hold period, the connection between the right side of the frontal region and the left side of the central region weakened, while between the middle of the frontal region and the middle of the occipital region strengthened. At this period, compared to palmer grasp, there was significantly higher connection strength in each brain region for lateral grasp. At the end of the movement, the connection between the right side of the frontal region and the left side of the central region strengthened.

In Figure 9b, it can be observed that in the beta band, there were consistently existing connections between the middle frontal region and the middle parietal region, as well as between the middle central region and the middle and right side of the parietal region at the rest state. In comparison with the rest state, the strength of the network connections on the left side of the frontal region was enhanced during the movement preparation period. At the onset of movement, the strength of the connection on the left side of the central region weakened. The connection between the right side of the central region and the left side of the parietal region weakened at the initiation of the grasp, along with a decrease in its connectivity strength. Meanwhile, the connection between the right side of the central region and the middle of the parietal region weakened for palmar grasp, while the connection between the left side of the parietal region and the occipital region weakened for lateral grasp. During the grasp-hold period, the connection between the left side of the central region and the occipital region weakened. At the end of the movement, the

connection between the left side of the central region and the occipital region strengthened.

V. DISCUSSION

In this paper, the brain functional connectivity of EEG during the movement state was investigated using the TFCMI. It was observed that the alpha (8-13 Hz) and beta (20-30 Hz) bands were closely associated with the motor and cognitive behavior of the subjects, which is consistent with previous research [43]. Compared to the rest state, the network connections between the central and parietal regions were significantly weaker in the alpha band during the movement preparation period, particularly in the left side of the brain. Conversely, in the beta band, the network connections between the left side of the parietal region and the left side of the frontal region, as well as between the left side of the parietal region and the right side of the central region, were enhanced. This enhancement can be attributed to the subjects being instructed to focus on the grasping target during the motor preparation period, thus creating an external visual stimulus. It has been previously shown that the default mode network is activated in the absence of external stimuli [38], [39], whereas when subjects direct their attention to external stimuli, the default mode network is inhibited, and the Central-Execution-Network (CEN) becomes active [44]. Moreover, the increased coupling strength and network connectivity between frontal region and other brain regions in the beta band, in the presence of visual stimuli, may indicate effective communication during visual processing [45].

By analyzing the functional brain connections during grasp tasks, our research reveals that the information transfer process in the brain relies on dynamic changes in the functional connections between brain regions. At the onset of the movement, the strength and number of network connections were significantly lower in the left-brain region compared to the right region. This apparent lateralization effect is consistent with the findings of previous studies on Event-Related-(De)Synchronization (ERDS) [46]. This lateralization effect aligns with previous studies on ERDS [46]. In the alpha band, the connection between the left and right side of the frontal region which used amplitude information, as well as between the left side of the frontal region and the right side of the parietal region using phase information, was consistently observed. In the beta band, it could be consistently observed that the connection between the central frontal region and the right side of the parietal region. These findings are attributed to the increased emphasis on the motor task at the onset of the movement, relative to visual stimuli during the preparation period, leading to the suppression of default mode network and activation of the central executive network to perform the grasp task. Throughout the entire movement, the frontal region remained active, highlighting its involvement in visual processing. The connections in the central region were more active during palmar grasp, whereas the connections in the parietal region were more active during lateral grasp. This suggests that both central and parietal regions contribute to

motor activity of the limbs, while the parietal region has a more refined control over limb movements. Furthermore, the strength of the connections between brain regions underwent dynamic of change throughout the movement, either strengthening or weakening. This demonstrates that the activation mechanism of the target brain region can be achieved not only by enhancing network connectivity, but also by reducing network connectivity.

It should be noted that the brain functional connectivity network investigated in this study is non-directional. Consequently, the causal relationship of network connections between brain regions throughout the entire motor process cannot be determined. Furthermore, there is no strict time requirement for the completion time of each motor period by the subjects in the dataset. Only sensors were used for calibration, resulting in some errors in dividing the motor period, which may have an impact on the analysis of the brain functional connection network during the motor task.

VI. CONCLUSION

In this study, the dynamic changes of the brain functional connectivity during grasp tasks were investigated using the TFCMI. Our findings revealed that the brain information transfer mechanism occurs through the reorganization of the brain functional connectivity. By incorporating attention and cognitive processes into the analysis of motor preparation, the dynamic changes of brain functional connectivity throughout the motor process were made more coherent and reasonable. There is a lateralization effect of the brain functional connectivity network at the onset of movement, which was associated with the hand used for motor execution (left or right). Compared to the default connectivity network observed during the rest state, clear evidence of reorganization in the brain functional connectivity network was observed throughout the movement. Notably, the reorganization processes exhibited significant differences across three movement tasks. These results provide valuable insights into the information exchange process between brain regions in real-motion scenarios. They also offer a theoretical foundation for the control of intelligent assistive devices using real-motion-related EEG signals, as well as new perspectives for the development and application of Brain-Computer-Interface (BCI) intelligent assistive devices.

REFERENCES

- [1] D. A. Abrams, C. J. Lynch, K. M. Cheng, J. Phillips, K. Supekar, S. Ryali, L. Q. Uddin, and V. Menon, "Underconnectivity between voice-selective cortex and reward circuitry in children with autism," *Proc. Nat. Acad. Sci. USA*, vol. 110, no. 29, pp. 12060–12065, Jul. 2013.
- [2] E. van Diessen, T. Numan, E. Van Dellen, A. W. Van Der Kooij, M. Boersma, D. Hofman, R. Van Lutterveld, B. W. Van Dijk, E. C. W. Van Straaten, A. Hillebrand, and C. J. Stam, "Opportunities and methodological challenges in EEG and MEG resting state functional brain network research," *Clin. Neurophysiol.*, vol. 126, no. 8, pp. 1468–1481, Aug. 2015.
- [3] B. He, L. Astolfi, P. A. Valdés-Sosa, D. Marinazzo, S. O. Palva, C.-G. Bénar, C. M. Michel, and T. Koenig, "Electrophysiological brain connectivity: Theory and implementation," *IEEE Trans. Biomed. Eng.*, vol. 66, no. 7, pp. 2115–2137, Jul. 2019.
- [4] W. Zhang, X. Han, S. Qiu, T. Li, C. Chu, L. Wang, J. Wang, Z. Zhang, R. Wang, M. Yang, X. Shen, Z. Li, L. Bai, Z. Li, R. Zhang, Y. Wang, C. Liu, and X. Zhu, "Analysis of brain functional network based on EEG signals for early-stage Parkinson's disease detection," *IEEE Access*, vol. 10, pp. 21347–21358, 2022.
- [5] Y. Wang, X. Chen, B. Liu, W. Liu, and R. M. Shiffrin, "Understanding the relationship between human brain structure and function by predicting the structural connectivity from functional connectivity," *IEEE Access*, vol. 8, pp. 209926–209938, 2020.
- [6] Y. Shi, W. Zeng, and S. Guo, "The occupational brain plasticity study using dynamic functional connectivity between multi-networks: Take seafarers for example," *IEEE Access*, vol. 7, pp. 148098–148107, 2019.
- [7] E. W. Pang and O. C. Snead III, "From structure to circuits: The contribution of MEG connectivity studies to functional neurosurgery," *Frontiers Neuroanatomy*, vol. 10, p. 67, Jun. 2016.
- [8] N. Xu, W. Shan, J. Qi, J. Wu, and Q. Wang, "Presurgical evaluation of epilepsy using resting-state MEG functional connectivity," *Frontiers Hum. Neurosci.*, vol. 15, Jul. 2021, Art. no. 649074.
- [9] P. Pantano, N. Petsas, F. Tona, and E. Sbardella, "The role of fMRI to assess plasticity of the motor system in MS," *Frontiers Neurol.*, vol. 6, p. 55, Mar. 2015.
- [10] Z. Chen, Z. Fu, and V. Calhoun, "Phase fMRI reveals more sparseness and balance of rest brain functional connectivity than magnitude fMRI," *Frontiers Neurosci.*, vol. 13, p. 204, Mar. 2019.
- [11] F. T. Sun, L. M. Miller, and M. D'Esposito, "Measuring interregional functional connectivity using coherence and partial coherence analyses of fMRI data," *NeuroImage*, vol. 21, no. 2, pp. 647–658, Feb. 2004.
- [12] A. Guillot, C. Collet, V. A. Nguyen, F. Malouin, C. Richards, and J. Doyon, "Brain activity during visual versus kinesthetic imagery: An fMRI study," *Hum. Brain Mapping*, vol. 30, no. 7, pp. 2157–2172, Jul. 2009.
- [13] Z. Fodor, A. Horváth, Z. Hidasi, A. A. Gouw, C. J. Stam, and G. Csukly, "EEG alpha and beta band functional connectivity and network structure mark hub overload in mild cognitive impairment during memory maintenance," *Frontiers Aging Neurosci.*, vol. 13, Oct. 2021, Art. no. 680200.
- [14] J. Zhang, "EEG-based sleep staging analysis with functional connectivity," *Int. J. Psychophysiol.*, vol. 168, p. S32, Oct. 2021.
- [15] M. Nentwich, L. Ai, J. Madsen, Q. K. Telesford, S. Haufe, M. P. Milham, and L. C. Parra, "Functional connectivity of EEG is subject-specific, associated with phenotype, and different from fMRI," *NeuroImage*, vol. 218, Sep. 2020, Art. no. 117001.
- [16] F. Di Gregorio and S. Battaglia, "Advances in EEG-based functional connectivity approaches to the study of the central nervous system in health and disease," *Adv. Clin. Experim. Med.*, vol. 32, no. 6, pp. 607–612, Jun. 2023.
- [17] G. Chiarion, L. Sparacino, Y. Antonacci, L. Faes, and L. Mesin, "Connectivity analysis in EEG data: A tutorial review of the state of the art and emerging trends," *Bioengineering*, vol. 10, no. 3, p. 372, Mar. 2023.
- [18] W. Xie, R. T. Toll, and C. A. Nelson, "EEG functional connectivity analysis in the source space," *Develop. Cognit. Neurosci.*, vol. 56, Aug. 2022, Art. no. 101119.
- [19] X. Li, J. Zhang, X.-D. Li, W. Cui, and R. Su, "Neurofeedback training for brain functional connectivity improvement in mild cognitive impairment," *J. Med. Biol. Eng.*, vol. 40, no. 4, pp. 484–495, Aug. 2020.
- [20] V. P. Varshney, N. Liapounova, A.-M. Golestani, B. Goodyear, and J. F. Dunn, "Detection of inter-hemispheric functional connectivity in motor cortex with coherence analysis," *J. Eur. Opt. Soc., Rapid Publications*, vol. 7, Nov. 2012.
- [21] M. Kaminski and K. J. Blinowska, "From coherence to multivariate causal estimators of EEG connectivity," *Frontiers Physiol.*, vol. 13, Apr. 2022, Art. no. 868294.
- [22] L. di Biase, L. Ricci, M. L. Caminiti, P. M. Pecoraro, S. P. Carbone, and V. Di Lazzaro, "Quantitative high density EEG brain connectivity evaluation in Parkinson's disease: The phase locking value (PLV)," *J. Clin. Med.*, vol. 12, no. 4, p. 1450, Feb. 2023.
- [23] S. Ashrafulla, J. P. Haldar, A. A. Joshi, and R. M. Leahy, "Canonical Granger causality between regions of interest," *NeuroImage*, vol. 83, pp. 99–189, Dec. 2013.
- [24] M. H. I. Shovon, N. Nandagopal, R. Vijayalakshmi, J. T. Du, and B. Cocks, "Directed connectivity analysis of functional brain networks during cognitive activity using transfer entropy," *Neural Process. Lett.*, vol. 45, no. 3, pp. 807–824, Jun. 2017.

- [25] B. L. Walker and K. A. Newhall, "Inferring information flow in spike-train data sets using a trial-shuffle method," *PLoS ONE*, vol. 13, no. 11, Nov. 2018, Art. no. e0206977.
- [26] L. Novelli and J. T. Lizier, "Inferring network properties from time series using transfer entropy and mutual information: Validation of multivariate versus bivariate approaches," *Netw. Neurosci.*, vol. 5, no. 2, pp. 373–404, 2021.
- [27] M. Celotto, S. Lemke, and S. Panzeri, "Inferring the temporal evolution of synaptic weights from dynamic functional connectivity," *Brain Informat.*, vol. 29, no. 1, p. 28, Dec. 2022.
- [28] C. C. Chen, J. C. Hsieh, Y. Z. Wu, P. L. Lee, S. S. Chen, D. M. Niddam, T. C. Yeh, and Y. T. Wu, "Mutual-information-based approach for neural connectivity during self-paced finger lifting task," *Hum. Brain Mapping*, vol. 29, no. 3, pp. 265–280, Mar. 2008.
- [29] C. F. Lu, S. Teng, C. I. Hung, P. J. Tseng, L. T. Lin, P. L. Lee, and Y. T. Wu, "Reorganization of functional connectivity during the motor task using EEG time-frequency cross mutual information analysis," *Clin. Neurophysiol.*, vol. 122, no. 8, pp. 1569–1579, Aug. 2011.
- [30] A. Gong, J. Liu, S. Chen, and Y. Fu, "Time-frequency cross mutual information analysis of the brain functional networks underlying multiclass motor imagery," *J. Motor Behav.*, vol. 50, no. 3, pp. 254–267, May 2018.
- [31] C. E. Shannon, "A mathematical theory of communication," *Bell Syst. Tech. J.*, vol. 27, no. 3, pp. 379–423, Jul. 1948.
- [32] T. E. Duncan, "On the calculation of mutual information," *SIAM J. Appl. Math.*, vol. 19, no. 1, pp. 215–220, Jul. 1970.
- [33] V. Bostanov, "BCI competition 2003—Data sets Ib and IIb: Feature extraction from event-related brain potentials with the continuous wavelet transform and the t-value scalogram," *IEEE Trans. Biomed. Eng.*, vol. 51, no. 6, pp. 1057–1061, Jun. 2004.
- [34] A. M. Fraser and H. L. Swinney, "Independent coordinates for strange attractors from mutual information," *Phys. Rev. A, Gen. Phys.*, vol. 33, no. 2, pp. 1134–1140, Feb. 1986.
- [35] K.-R. Müller, M. Krauledat, G. Dornhege, G. Curio, and B. Blankertz, "Machine learning techniques for brain-computer interfaces," *Biomed. Tech.*, vol. 49, no. 1, pp. 11–22, Dec. 2004.
- [36] M. Rubinov and O. Sporns, "Complex network measures of brain connectivity: Uses and interpretations," *NeuroImage*, vol. 52, no. 3, pp. 1059–1069, Sep. 2010.
- [37] T. Adamovich, I. Zakharov, A. Tabueva, and S. Malykh, "The thresholding problem and variability in the EEG graph network parameters," *Sci. Rep.*, vol. 12, no. 1, p. 18659, Nov. 2022.
- [38] R. L. Buckner, J. R. Andrews-Hanna, and D. L. Schacter, "The brain's default network: Anatomy, function, and relevance to disease," in *Year in Cognitive Neuroscience*, vol. 1124, A. Kingstone and M. B. Miller, Eds. New York, NY, USA: Academy of Sciences, 2008, pp. 1–38.
- [39] J. R. Andrews-Hanna, J. S. Reidler, J. Sepulcre, R. Poulin, and R. L. Buckner, "Functional-anatomic fractionation of the brain's default network," *Neuron*, vol. 65, no. 4, pp. 550–562, Feb. 2010.
- [40] A. Schwarz, C. Escolano, L. Montesano, and G. R. Müller-Putz, "Analyzing and decoding natural reach-and-grasp actions using gel, water and dry EEG systems," *Frontiers Neurosci.*, vol. 14, p. 849, Aug. 2020.
- [41] A. Hyvärinen and E. Oja, "Independent component analysis: Algorithms and applications," *Neural Netw.*, vol. 13, nos. 4–5, pp. 411–430, Jun. 2000.
- [42] B. Hjorth, "Principles for transformation of scalp EEG from potential field into source distribution," *J. Clin. Neurophysiol.*, vol. 8, no. 4, pp. 391–396, 1991.
- [43] G. Pfurtscheller, A. Stancák, and C. Neuper, "Event-related synchronization (ERS) in the alpha band—An electrophysiological correlate of cortical idling: A review," *Int. J. Psychophysiology*, vol. 24, nos. 1–2, pp. 39–46, Nov. 1996.
- [44] Y. I. Sheline, J. L. Price, Z. Yan, and M. A. Mintun, "Resting-state functional MRI in depression unmasks increased connectivity between networks via the dorsal Nexus," *Proc. Nat. Acad. Sci. USA*, vol. 107, no. 24, pp. 11020–11025, 2010.
- [45] P. Sehatpour, S. Molholm, T. H. Schwartz, J. R. Mahoney, A. D. Mehta, D. C. Javitt, P. K. Stanton, and J. J. Foxe, "A human intracranial study of long-range oscillatory coherence across a frontal-occipital-hippocampal brain network during visual object processing," *Proc. Nat. Acad. Sci. USA*, vol. 105, no. 11, pp. 4399–4404, 2008.
- [46] G. Mueller-Putz, R. Scherer, G. Pfurtscheller, and C. Neuper, "Temporal coding of brain patterns for direct limb control in humans," *Frontiers Neurosci.*, vol. 4, p. 1170, Jun. 2010.

HAO GU received the B.E. degree from the North University of China, Taiyuan, China, in 2015, where he is currently pursuing the Ph.D. degree in information and communication engineering. His research interests include EEG signal processing and machine learning.

JIAN WANG received the master's degree in signal and information processing from the North University of China, Taiyuan, China, in 2005, where she is currently pursuing the Ph.D. degree in information and communication engineering. Her research interest includes signal processing.

YAN HAN received the Ph.D. degree in signal and information processing from the Beijing Institute of Technology, Beijing, China, in 1998. He is currently a Professor with the North University of China. His research interests include signal processing, non-destructive testing, and image processing.

• • •